⌘ *Author's Choice*

THE JOURNAL OF BIOLOGICAL CHEMISTRY VOL. 284, NO. 7, pp. 4705–4712, February 13, 2009

The N-terminal Amphipathic α-Helix of Viperin Mediates Localization to the Cytosolic Face of the Endoplasmic Reticulum and Inhibits Protein Secretion*[S]

Received for publication, September 18, 2008, and in revised form, December 11, 2008 Published, JBC Papers in Press, December 12, 2008, DOI 10.1074/jbc.M807261200

Ella R. Hinson[‡] **and Peter Cresswell**[§¶1]

From the [‡]*Section of Microbial Pathogenesis,* [§]*Department of Immunobiology, and* [¶]*Howard Hughes Medical Institute, Yale University School of Medicine, New Haven, Connecticut 06520-8011*

Viperin is an evolutionarily conserved interferon-inducible protein that localizes to the endoplasmic reticulum (ER) and inhibits a number of DNA and RNA viruses. In this study, we report that viperin specifically localizes to the cytoplasmic face of the ER and that an amphipathic α-helix at its N terminus is necessary for the ER localization of viperin and sufficient to promote ER localization of a reporter protein, dsRed. Overexpression of intact viperin but not the amphipathic α-helix fused to dsRed induced crystalloid ER. Consistent with other proteins that induce crystalloid ER, viperin self-associates, and it does so independently of the amphipathic α-helix. Viperin expression also affected the transport of soluble but not membrane-associated proteins. Expression of intact viperin or an N-terminal α-helix-dsRed fusion protein significantly reduced secretion of soluble alkaline phosphatase and reduced its rate of ER-to-Golgi trafficking. Similarly, viperin expression inhibited bulk protein secretion and secretion of endogenous α_1-antitrypsin and serum albumin from HepG2 cells. Converting hydrophobic residues in the N-terminal α-helix to acidic residues partially or completely restored normal transport of soluble alkaline phosphatase, suggesting that the extended amphipathic nature of the N-terminal α-helical domain is essential for inhibiting protein secretion.

Type I interferons are the first line of defense against viral infections. The significance of the interferon pathway is illustrated by the susceptibility of interferon signaling mutants to infection and by viral mechanisms that counteract this pathway (1, 2). Although many genes are induced upon interferon stimulation, very few of these genes have been functionally characterized. Viperin is highly induced by both Type I and II interferons and has a broad range of antiviral activity, inhibiting DNA viruses, notably human cytomegalovirus (3); RNA viruses such as influenza, hepatitis C virus (HCV),[2] and alphaviruses (4–6); and retroviruses such as human immunodeficiency virus (7). Upon expression, viperin localizes to the endoplasmic reticulum (ER), where it interacts with farnesyl-diphosphate synthase, an enzyme involved in lipid biosynthesis. This interaction appears to result in the disruption of lipid raft microdomains and prevention of influenza virus from budding from the plasma membrane (4).

Although recent studies have explored the antiviral functions of viperin, the general biochemical properties of this protein remain largely undefined. Viperin is highly conserved across both mammals and lower vertebrates and shares homology with the MoaA family of "radical *S*-adenosylmethionine" enzymes that bind Fe-S clusters (3, 8). In addition to a putative Fe-S cluster-binding domain, viperin has a 42-amino acid residue N-terminal amphipathic α-helix, and similar domains in other proteins have been shown to bind membranes and induce membrane curvature (9, 10).

In this study, we examined the role of the viperin N-terminal α-helical domain in both cellular localization and ER membrane morphology and analyzed the biochemical properties of viperin. We discovered that viperin forms dimers and induces a tightly ordered, visually striking array of ER membranes, known as crystalloid ER(11–13), upon overexpression. In addition, viperin expression impedes the secretion of a variety of soluble proteins. Although the N-terminal amphipathic α-helix is not sufficient to induce crystalloid ER formation, it is both necessary and sufficient to mediate ER localization and to inhibit protein secretion.

EXPERIMENTAL PROCEDURES

Cells, Antibodies, and Constructs—HepG2, HeLa, and 293T cells were maintained in Dulbecco's modified Eagle's medium containing 5% bovine calf serum. The following antibodies were purchased commercially: anti-placental alkaline phosphatase (ab11299), anti-α_1-antitrypsin (ab7633), anti-human serum albumin (ab18079), and anti-Myc (ab9106) (Abcam) and anti-hemagglutinin (HA) tag (HA.11; Covance). MaP.VIP and rabbit anti-calnexin antibody (4) and the mouse anti-tapasin monoclonal antibody PaSta1(14) were described previously. Goat anti-rabbit and anti-mouse Ig secondary antibodies were purchased commercially from Molecular Probes. All viperin constructs were generated by PCR amplification and then cloned into pcDNA3.1. The dsRed gene cassette was excised from pDsRed-Monomer (Clontech) using restriction enzyme digestion and then cloned into pcDNA3.1 with or without res-

* The work was supported by the Ellison Foundation and the Howard Hughes Medical Institute. The costs of publication of this article were defrayed in part by the payment of page charges. This article must therefore be hereby marked "*advertisement*" in accordance with 18 U.S.C. Section 1734 solely to indicate this fact.

⌘ *Author's Choice*—Final version full access.

[S] The on-line version of this article (available at http://www.jbc.org) contains supplemental Figs. 1–3.

[1] To whom correspondence should be addressed: Dept. of Immunobiology, Yale University School of Medicine, 300 Cedar St., TAC S670, New Haven, CT 06520-8011. Fax: 203-737-1764; E-mail: peter.cresswell@yale.edu.

[2] The abbreviations used are: HCV, hepatitis C virus; ER, endoplasmic reticulum; HA, hemagglutinin; SeAP, secreted alkaline phosphatase; WT, wild-type.

idues 1–42 of viperin. The pRSVPAP construct, which encodes placental alkaline phosphatase, was purchased from American Type Culture Collection. The construct encoding TAP1 (transporter associated with antigen processing subunit 1) fused to Cherry at its C terminus was a kind gift from Dr. David Stepensky (Ben-Gurion University, Beersheba, Israel). Constructs encoding secreted alkaline phosphatase (SeAP) and Sar1 and Arf1 dominant negatives were kind gifts from Dr. Jon Kagan (Harvard University). The expression construct encoding the vesicular stomatitis virus glycoprotein temperature-sensitive ts045 mutant (15) was provided by Dr. Jennifer Lippincott-Schwartz (National Institutes of Health).

Transfection—Cells were transiently transfected using Lipofectamine 2000 (Invitrogen) following the manufacturer's instructions.

Western Blotting—Cells were harvested, washed once in phosphate-buffered saline, and lysed in 1% Triton X-100 in Tris-buffered saline (0.15 M NaCl and 0.01 M Tris, pH 7.4) containing a protease inhibitor mixture (Roche Applied Science). Whole cell lysates were separated by SDS-PAGE, transferred to polyvinylidene difluoride membranes (Millipore), and then probed with the indicated antibodies.

Immunofluorescence—HeLa cells or 293T cells transiently expressing wild-type (WT) viperin, viperin lacking the N-terminal amphipathic α-helix (viperin-(Δ1–42)), or viperin bearing mutations in the α-helix were plated onto glass coverslips. Forty-eight hours post-transfection, the cells were fixed in 4% formaldehyde, washed, permeabilized with 0.05% saponin or 0.1% Triton X-100, and stained with the indicated antibodies. For selective plasma membrane permeabilization, cells were treated with 22 μg/ml streptolysin O (Aalto) in the presence of 0.3 mM dithiothreitol for 15 min on ice, washed in intracellular transport buffer (50 mM HEPES, 78 mM KCl, 4 mM $MgCl_2$, 8.37 mM $CaCl_2$, and 10 mM EGTA), and incubated for 5 min at 37 °C. After permeabilization, cells were fixed in 4% formaldehyde and then stained with the indicated antibodies in intracellular transport buffer.

Electron Microscopy—293T cells transiently expressing the vector control, WT viperin, or viperin-(1–42)-dsRed were examined by electron microscopy as described previously (4). For immunoelectron microscopy, cells were fixed in 4% paraformaldehyde (Electron Microscopy Sciences) in 0.25 M HEPES, pH 7.4, for 1 h at room temperature and then in 8% paraformaldehyde in 0.25 M HEPES, pH 7.4, overnight at 4 °C. Samples were prepared for immunochemistry as described previously (16) and stained with MaP.VIP and 10 nm of protein A-gold (Cell Microscopy Center, Utrecht University, The Netherlands). Sections were examined with a Tecnai 12 Biotwin electron microscope, and images were captured using a charge-coupled device camera (Morada, Olympus).

SeAP Assay—293T cells were cotransfected with SeAP and the indicated viperin constructs. Twenty-four hours post-transfection, cell supernatants were harvested and analyzed for SeAP secretion by an alkaline phosphatase assay using the Phospha-Light system (Applied Biosystems) and a luminometer.

Radiolabeling and Pulse-Chase Analysis—Transiently transfected 293T cells or HepG2 cells were harvested, washed once in phosphate-buffered saline, and starved for 1 h in Dulbecco's modified Eagle's medium without methionine or cysteine (Sigma) containing 3% dialyzed fetal bovine serum. Cells were labeled for the indicated times with [^{35}S]methionine (PerkinElmer Life Sciences) and then chased with Dulbecco's modified Eagle's medium containing 10% bovine calf serum and excess methionine and cysteine. Cells and supernatants were harvested at the indicated times and stored at −20 °C until detergent lysis.

Immunoprecipitation—Cells were lysed in 1% Triton X-100 in Tris-buffered saline containing protease inhibitors for 30 min on ice. For radiolabeled cells, extracts were precleared with protein G-Sepharose (GE Healthcare) and normal rabbit serum and then immunoprecipitated with the indicated antibodies and protein G-Sepharose. Immunoprecipitates were washed, eluted in reducing sample buffer, run on SDS-polyacrylamide gels, dried, and exposed to PhosphorImager screens for quantification with ImageQuant software. For viperin co-immunoprecipitations, cell extracts were precleared with protein G-Sepharose, immunoprecipitated with anti-HA or control antibody, and then blotted with anti-Myc antibody.

RESULTS

The N-terminal Amphipathic α-Helix Is Necessary and Sufficient to Localize Viperin to the Cytoplasmic Face of the ER—Although previous studies have shown that viperin localizes to the ER, the precise topology and the ER localization signal of viperin were not identified. To determine whether viperin localizes to the cytosolic or lumenal face of the ER, we used streptolysin O to selectively permeabilize the plasma membrane, followed by staining with the anti-viperin monoclonal antibody MaP.VIP. An anti-tapasin antibody that recognizes a lumenal ER epitope and an anti-calnexin antibody that recognizes a cytosolic epitope were used as controls. Under these conditions, viperin and calnexin staining was readily observed, whereas the ER lumenal epitope of tapasin was detected only after saponin permeabilization (Fig. 1*A*). This demonstrated that viperin was localized to the cytosolic face of the ER. To identify the domain responsible, we focused on the N-terminal α-helix because it has a wide hydrophobic face that is characteristic of helices that not only bind to the ER but also induce membrane curvature. First, to determine whether the α-helix is necessary for ER localization, we used immunofluorescence to examine cells expressing WT viperin or a deletion mutant lacking this domain (viperin-(Δ1–42)). WT viperin colocalized with ER resident proteins, namely human TAP1 fused to the fluorescent protein tag Cherry and calnexin, but removing the α-helix relocalized viperin to the cytosol (Fig. 1*B*). Adding the N-terminal α-helix of viperin to dsRed was also sufficient to relocalize this reporter protein from the cytosol and nucleus to the ER (Fig. 1*C*).

Viperin Overexpression Induces Crystalloid ER—To confirm the ER localization of viperin, we used immunoelectron microscopy to examine 293T cells expressing viperin. We observed that these cells contained membranous structures highly similar to previously described crystalloid ER, characterized by the distortion of smooth ER membranes into a lattice-like pattern (Fig. 2*A*) (12, 13, 17). However, the amphipathic

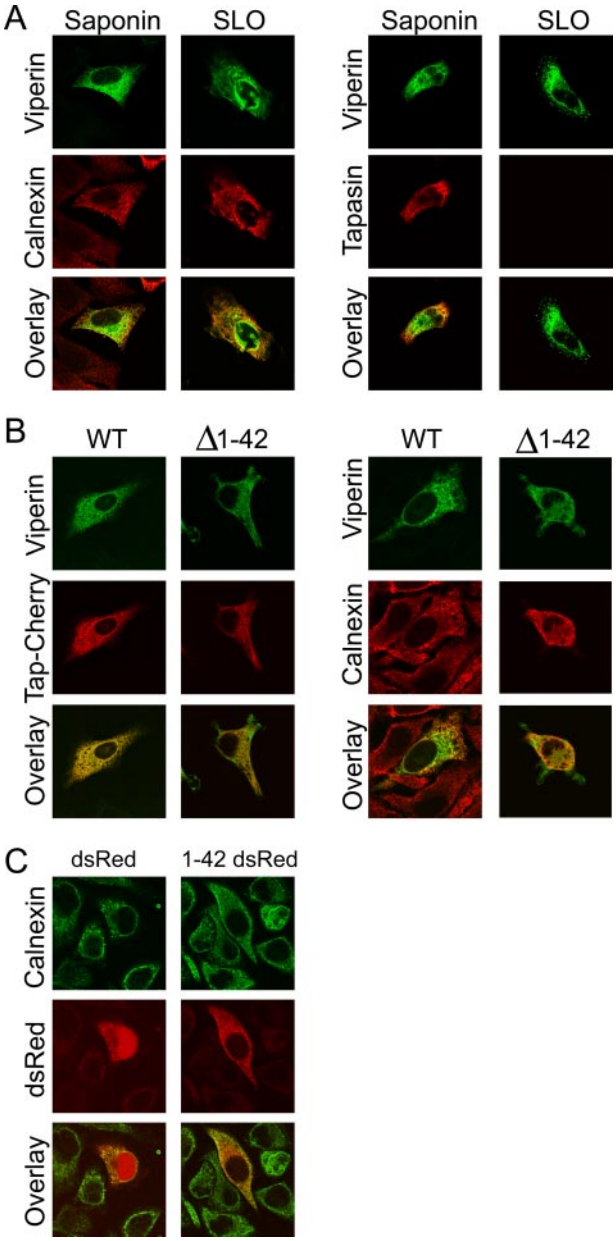

FIGURE 1. **Viperin localizes to the cytosolic face of the ER through its N-terminal amphipathic α-helix.** *A*, HeLa cells transiently expressing viperin and tapasin were treated with streptolysin O (*SLO*) to selectively permeabilize the plasma membrane or completely permeabilized with saponin. Cells were stained with the anti-viperin monoclonal antibody MaP.VIP and either an anti-tapasin antibody that recognizes a lumenal ER epitope or an anti-calnexin antibody that recognizes a cytosolic epitope. *B*, HeLa cells transiently expressing WT viperin or viperin-(Δ1–42) were analyzed for colocalization with TAP1-Cherry and endogenous calnexin. *C*, HeLa cells transiently expressing dsRed or viperin-(1–42)-dsRed were analyzed for colocalization with calnexin.

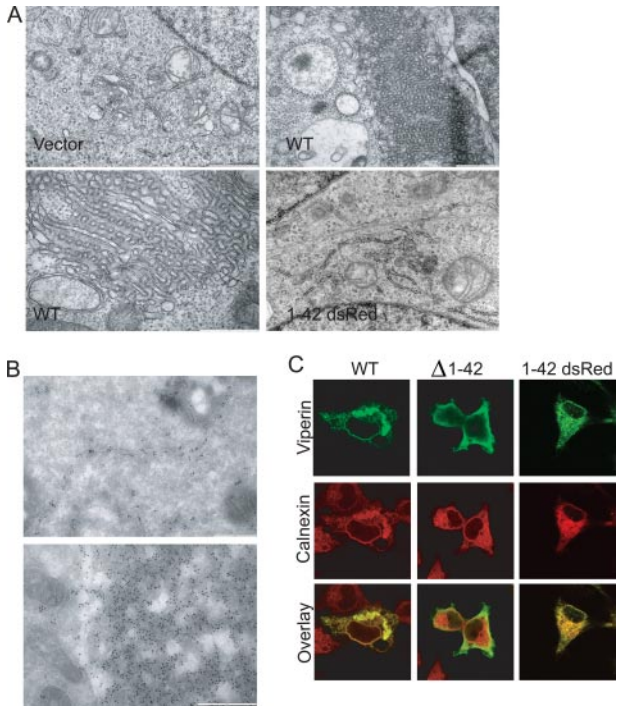

FIGURE 2. **Viperin expression distorts ER membranes.** 293T cells transiently expressing WT viperin or viperin-(1–42)-dsRed were analyzed by electron microscopy (*A*) and by immunoelectron microscopy with MaP.VIP (*B*) for viperin localization and ER membrane morphology. *Scale bar* = 1 μm for vector and viperin-(1–42)-dsRed images and 500 nm for WT images. 293T cells transiently expressing WT viperin, viperin-(Δ1–42), or viperin-(1–42)-dsRed were analyzed by immunofluorescence and co-stained with an antibody to the ER resident protein calnexin to examine the formation of crystalloid ER (*C*).

α-helix-dsRed fusion protein did not induce these morphological changes (Fig. 2*A*), indicating that the α-helical domain is not sufficient to induce crystalloid ER. Immunoelectron microscopy showed that viperin was highly concentrated in these membranous areas in addition to normal ER (Fig. 2*B*). Further analysis of viperin-expressing cells by immunofluorescence using Triton X-100 rather than saponin for permeabilization confirmed that expression of WT viperin but not viperin-(Δ1–42) or the α-helix-dsRed fusion protein induced dramatically distorted ER structures, defined by the presence of calnexin (Fig. 2*C*).

Viperin Forms Dimers Independently of the N-terminal Amphipathic α-Helix—Proteins that induce crystalloid ER are often dimeric (13), and we therefore wished to determine whether viperin is capable of dimerization. Using Myc- and HA-tagged viperin expression vectors, we overexpressed these proteins in 293T cells and performed co-immunoprecipitation studies on detergent extracts. HA-tagged viperin co-immunoprecipitated with Myc-tagged viperin but not with a Myc-tagged control protein, Rp14 (ribosomal protein 14) (Fig. 3). To determine whether this self-interaction requires the N-terminal amphipathic α-helix, we performed similar co-immunoprecipitations with HA- and Myc-tagged viperin-(Δ1–42) truncation mutants. The viperin mutants were also capable of self-association, indicating that viperin dimerization or multimerization can occur independently of the amphipathic α-helical domain (Fig. 3).

The N-terminal Amphipathic α-Helix Is Necessary and Sufficient to Inhibit Protein Secretion—To determine whether the viperin-induced morphological changes affected ER function, we examined protein trafficking in viperin-expressing cells. Viperin expression in HepG2 cells caused a reduction in protein secretion, as measured by the amount of ^{35}S-labeled proteins secreted into the supernatant normalized to the total amount of ^{35}S-labeled proteins in whole cell extracts. Although expression of the green fluorescent protein control had no

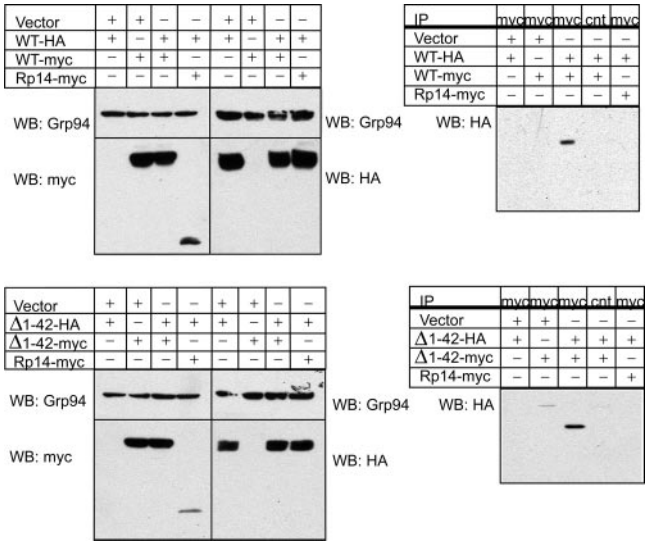

FIGURE 3. **Viperin self-interacts independently of the N-terminal amphipathic α-helix.** 293T cells were transiently transfected with HA- and Myc-tagged WT viperin or viperin-(Δ1–42), lysed, and then examined by Western blotting (*WB*) for protein expression and by co-immunoprecipitation (*IP*) with a control or anti-HA antibody for protein dimerization. Rp14-Myc served as a negative control, and Grp94 served as a protein loading control.

effect on protein secretion relative to the vector control, viperin expression reduced total protein secretion from HepG2 cells to levels comparable with those observed in cells expressing dominant-negative Sar1 and Arf1 (Fig. 4*A*, *Sar1dn* and *Arf1dn*) previously shown to dramatically affect protein secretion (18, 19). By combining pulse-chase analysis and immunoprecipitations from cell supernatants and extracts, we specifically examined the secretion of endogenous albumin (Fig. 4*B*), α_1-antitrypsin (Fig. 4*C*), and transferrin (data not shown) by ^{35}S-labeled HepG2 cells and found that secretion of all three of these soluble proteins was significantly reduced in viperin-expressing cells.

To determine whether the reduction in protein secretion was a direct consequence of crystalloid ER formation or a separate function associated with the N-terminal amphipathic α-helix, we cotransfected various constructs into 293T cells along with the secreted version of placental alkaline phosphatase lacking the membrane anchor (SeAP) (20). SeAP secretion was assayed enzymatically, and intracellular transport was assessed using pulse-chase radiolabeling, immunoprecipitation, and endoglycosidase H digestion. The N-terminal amphipathic α-helix (amino acids 1–42) alone was able to reduce SeAP secretion to levels comparable with WT viperin, whereas secretion in cells expressing viperin-(Δ1–42) was comparable with that in cells expressing the vector control or the control protein Rp14 (Fig. 5*A*). Pulse-chase analysis of SeAP showed that that the amphipathic α-helical domain was both necessary and sufficient to inhibit the ER-to-Golgi trafficking of SeAP, measured by the rate of acquisition of endoglycosidase H resistance (Fig. 5*B*). Furthermore, the N-terminal amphipathic α-helix fused to monomeric dsRed also inhibited SeAP secretion and significantly delayed the acquisition of endoglycosidase H resistance compared with the vector control or dsRed alone (Fig. 5, *C* and *D*).

Although viperin expression affected the secretion of soluble proteins, there was no discernible effect on the intracellular trafficking rates of membrane-bound proteins. Using a temperature-sensitive variant of vesicular stomatitis virus glycoprotein (ts045), we found that the rate at which vesicular stomatitis virus glycoprotein arrived at the cell surface after shifting to the permissive temperature was comparable in viperin-expressing and control cells (supplemental Fig. 1*A*). Similarly, the rate at which placental alkaline phosphatase (PLAP), the glycosylphosphatidylinositol-anchored protein that is truncated before the transmembrane domain to yield the soluble SeAP reporter (20), arrived at the cell surface was unaffected in viperin-expressing cells (supplemental Fig. 1*B*). However, transport was significantly delayed by expression of the dominant-negative version of Sar1. Furthermore, viperin expression did not alter the ER-to-Golgi trafficking rates of vesicular stomatitis virus glycoprotein (data not shown) or placental alkaline phosphatase, as measured by the acquisition of endoglycosidase H resistance in radiolabel pulse-chase experiments, whereas dominant-negative versions of Sar1 and Arf1 effectively reduced the transport rate (supplemental Fig. 1*C*).

Mutating Hydrophobic Residues in the Amphipathic α-Helix Restores Protein Secretion—Arrangement of the N-terminal domain of viperin into a helical wheel showed the classic amphipathic arrangement of residues, with hydrophobic amino acids localized on an extended face of the α-helix (Fig. 6*A*). To determine whether this face of the α-helix is involved in inhibiting protein secretion, specific hydrophobic residues were mutated to alanine or glutamic acid (*circled* in Fig. 6*A*), and charged arginine residues were mutated to serine (*pink* in Fig. 6*A*). Although mutating hydrophobic residues to alanine or charged arginine residues to serine did not alter the ability of viperin to inhibit protein secretion (data not shown), mutating hydrophobic residues to glutamic acid partially or completely restored protein secretion (Fig. 6*B*). Although none of the single glutamic acid substitutions affected the ER localization of viperin (supplemental Fig. 2), mutating three hydrophobic residues to glutamic acid disrupted ER association (Fig. 6*C*). In addition, sequentially deleting turns in the α-helix disrupted ER association, resulting in the progressive relocalization of viperin to the cytosol (supplemental Fig. 3).

DISCUSSION

Viperin has a broad range of antiviral activity and is highly conserved in evolution, suggesting that it is functionally extremely important. As is the case for other interferon-induced antiviral proteins, the precise mechanism(s) of action of viperin remains largely unknown. To date, the only mechanistic information indicates an effect of viperin expression on lipid raft microdomains and a potential role for the conserved putative Fe-S-binding motif in HCV infection (4, 8). In this study, we identified and examined the properties of the different domains of viperin. We showed that a region in the C-terminal domain is important for protein dimerization and that the N-terminal amphipathic α-helical domain is required for ER localization and interferes with the secretion of soluble proteins.

Overexpression of viperin induced dramatic changes in ER morphology that are characteristic of crystalloid ER. Crystal-

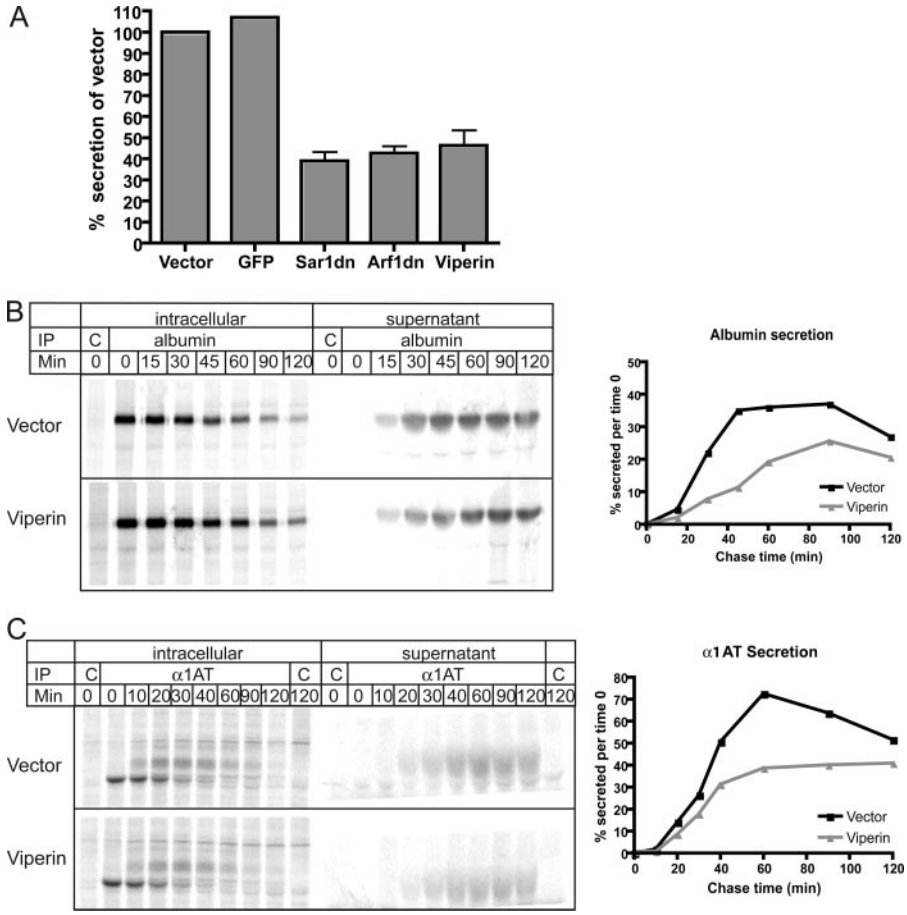

FIGURE 4. **Viperin reduces protein secretion by HepG2 cells.** *A*, HepG2 cells expressing the indicated proteins were radiolabeled with [^{35}S]methionine for 1 h and then chased for 2 h. The amount of total ^{35}S-labeled protein secreted into the supernatant was normalized to the total amount of labeled proteins in cell extracts. Vector and green fluorescent protein (*GFP*) served as negative controls, whereas dominant-negative Sar1 (*Sar1dn*) and Arf1 (*Arf1dn*) served as positive controls. The graph represents an average of three independent experiments. *B* and *C*, HepG2 cells expressing viperin or the vector control were [^{35}S]methionine-labeled for 10 min and then chased for the indicated times. Supernatants and cell extracts were immunoprecipitated (*IP*) with control antibodies (*C*) or antibodies to albumin (*B*) or α_1-antitrypsin (*α1AT*) (*C*). Graphs on the right show the percent of protein secreted normalized to the total amount of protein at time 0. These results are representative of at least three independent experiments.

loid ER is induced by a number of membrane-associated proteins (11, 13). Current models for crystalloid ER formation propose that smooth ER is morphologically altered when the cytoplasmic domains of ER-bound proteins form high affinity dimers and bring apposing membranes together to form a lattice-like pattern of hexagonally packed tubules (11–13). Consistent with this model, we showed that viperin self-interacts to form multimers, likely to be dimers. The interaction occurred in viperin truncation mutants lacking the amphipathic α-helix, arguing that it is independent of the ER localization domain. However, preliminary size exclusion data (data not shown) obtained with purified, soluble, recombinant viperin lacking the N-terminal α-helical domain suggest that the extent of dimerization is low in solution; membrane association may enhance the tendency to multimerize by limiting movement to the plane of the membrane. We did not find that viperin expression and crystalloid ER formation induced the unfolded protein response, based on analysis of XBP-1 mRNA processing (data not shown) (21).

Although crystalloid ER has dramatic effects on ER morphology, our data suggest that it is not responsible for the defects in protein secretion that we observed upon viperin expression. We also failed to find any effects on steady-state levels or localization of a number of ER resident proteins, including tapasin, calnexin, ERp57, and Grp94 (data not shown). Expressing a fusion protein containing the amphipathic α-helix N-terminal to monomeric dsRed did not induce crystalloid ER formation but still inhibited protein secretion to a level comparable with that observed with WT viperin. We hypothesize that the N-terminal amphipathic α-helix induces localized membrane curvature that is further exacerbated upon viperin dimerization via its C terminus to cause crystalloid ER formation. Previous reports have shown that amphipathic α-helices modulate membrane curvature (9, 10, 22). Specifically, amphipathic α-helices with wide hydrophobic faces, notably Sar1, localize to the ER and induce membrane curvature (9, 23). When specific hydrophobic residues on the Sar1 helical wheel were changed to alanine, the mutant Sar1 proteins induced altered membrane tubulation and affected the size of liposomes generated *in vitro* in association with Sar1 (23). Our mutational analysis of the amphipathic α-helix of viperin showed that more dramatic changes were required to observe an effect on secretion in that the hydrophobic residues needed to be changed to charged glutamic acid residues rather than alanine residues. This may be because the amphipathic α-helix of viperin, which consists of 42 amino acids compared with 23 residues in the case of Sar1, has a more extended hydrophobic face. Also compatible with this idea is the observation that more than four helical turns had to be deleted or at least three hydrophobic residues had to be mutated to glutamic acid to induce dissociation of viperin from the ER membrane.

Crystalloid ER formation upon viperin expression is consistent with an increase in membrane curvature of the ER, which may be caused by the amphipathic α-helix and exacerbated by viperin dimerization. It is tempting to infer that the increase in membrane curvature is also responsible for the reduction in protein secretion that is observed upon expression of viperin or the amphipathic α-helix linked to the marker protein dsRed. Although not demonstrated here, the association of viperin with secretory coat protein complex II (COPII) vesicles and an enhancement of membrane curvature caused by the α-helix could reduce the size of the vesicles. Geometric principles sug-

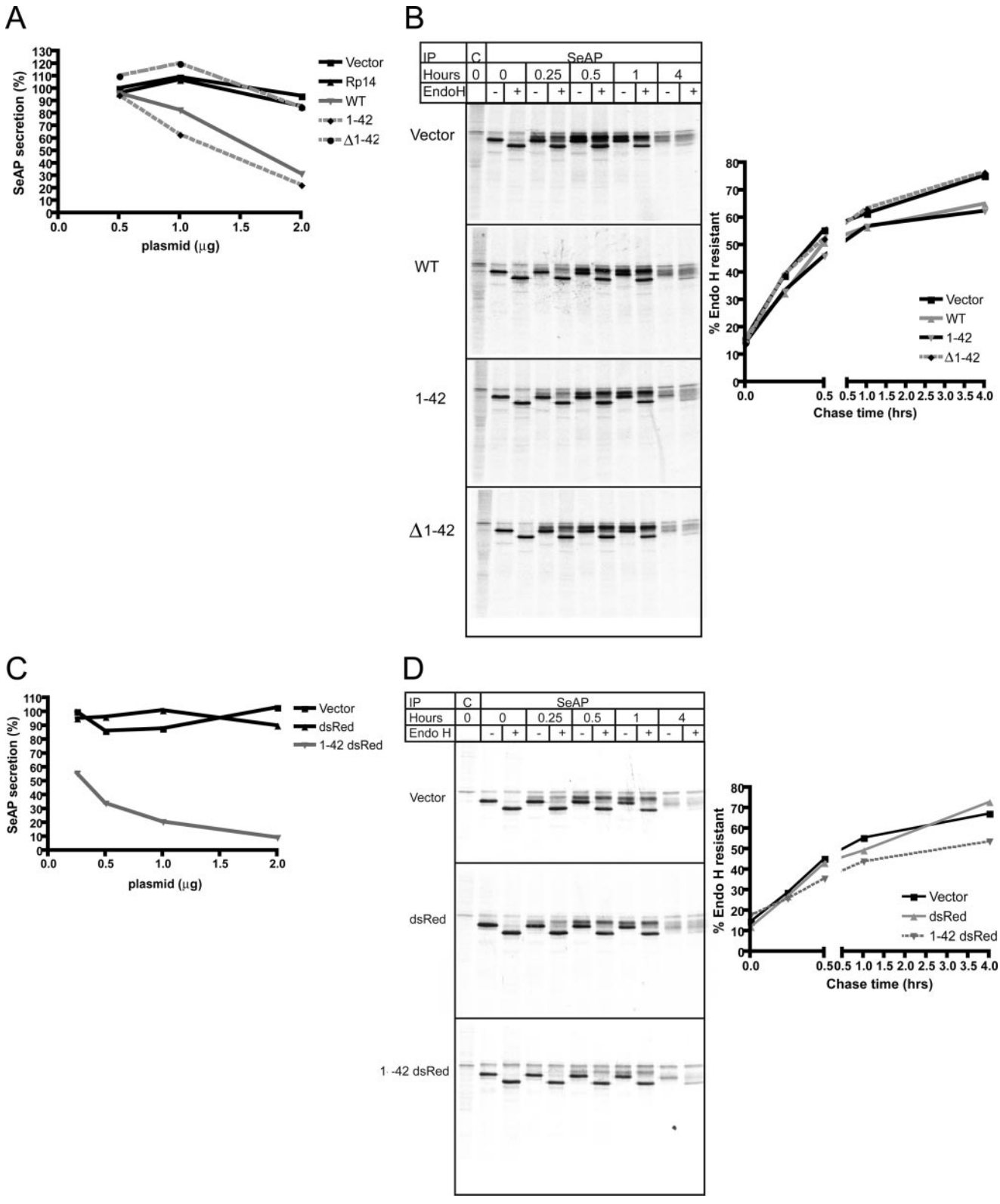

FIGURE 5. **The N-terminal amphipathic α-helix of viperin is necessary and sufficient to delay ER-to-Golgi trafficking of SeAP.** *A*, 293T cells were transiently transfected with SeAP and the indicated amounts of viperin or control constructs and then analyzed for SeAP secretion 24 h post-transfection. SeAP secretion is expressed as a percentage of the vector control at 0.5 μg of transfected DNA. *B*, 293T cells transiently expressing SeAP and the indicated constructs were [^{35}S]methionine-labeled for 10 min and then chased for the indicated times. 293T cell detergent lysates were immunoprecipitated (*IP*) with control (*C*) or anti-SeAP antibodies and then treated with endoglycosidase H (*Endo H*). The graph shows the percent of endoglycosidase H-resistant SeAP for each time point. *C*, SeAP secretion was examined as described for *A* with the indicated constructs. SeAP secretion is expressed as a percentage of the vector control at 0.25 μg of transfected DNA. *D*, the acquisition of SeAP endoglycosidase H resistance was examined as described for *B* with the indicated constructs. Each experiment is representative of at least three independent experiments.

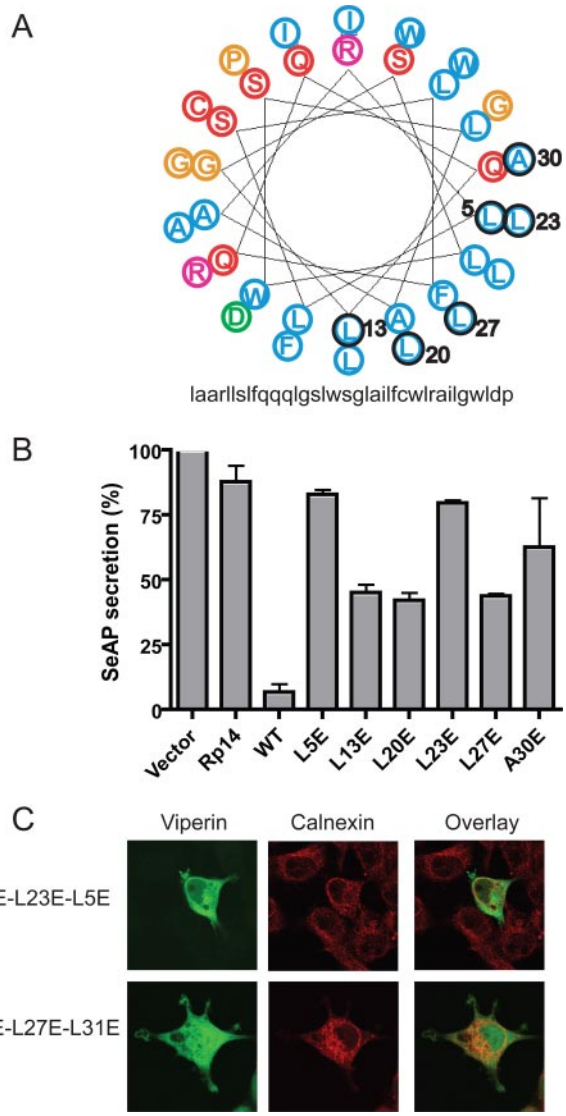

FIGURE 6. **Point mutants in the amphipathic α-helix restore SeAP secretion.** *A*, shown is a helical wheel diagram of residues 9–42 of the N-terminal amphipathic α-helix of viperin, with hydrophobic residues in *blue*, neutral potentially hydrogen-bonding residues in *red*, acidic residues in *green*, basic residues in *pink*, and other residues in *orange* (adapted from the Rutgers University Helical Wheel Drawing Program). The *numbered* residues outlined in *black* were mutated to glutamic acid. *B*, shown are the results from analysis of SeAP secretion as described in the legend to Fig. 2*A* with the indicated viperin helical wheel mutants. SeAP secretion is expressed as a percentage of the vector control. These results are representative of at least three independent experiments. *C*, 293T cells expressing amphipathic α-helix mutants with three hydrophobic residues mutated to glutamic acid were analyzed by immunofluorescence for ER localization using calnexin.

gest that a reduction in the volume of secretory vesicles induced by a reduction in curvature would reduce the incorporation of soluble cargo to a much greater extent than transmembrane cargo, which might explain the suppressive effect of viperin expression on the transport of soluble but not membrane-associated proteins. Unfortunately, attempts to purify recombinant WT viperin were unsuccessful, and therefore, we were unable to measure membrane curvature of viperin-associated liposomes *in vitro*. However, the similarities between the amphipathic α-helices of viperin and Sar1 suggest a similar mechanism of ER localization and potentially similar effects on membrane curvature. Alternative hypotheses for a viperin-induced reduction in soluble protein secretion but not membrane-associated proteins do exist, however. For example, viperin could differentially associate with vesicles bearing soluble or transmembrane cargo. Resolution of this question awaits additional experiments.

A key question is whether the viperin-induced effects on the ER could contribute to its antiviral activity. Viperin may inhibit the trafficking of soluble virally encoded and cellular proteins necessary for viral replication, and certain viruses also use membranes derived from the ER for viral replication, budding, and exit via the secretory route (24, 25). Therefore, one of the antiviral functions of viperin may be to prevent or alter the formation of these membranous complexes, thus affecting viral replication or egress. A previous report suggests that viperin inhibits HCV replication (5), which is known to generate a replication complex potentially derived from ER membranes. Future studies will investigate if viperin can specifically alter formation of the HCV replication complex and prevent HCV replication.

Although viperin shares significant homology with the MoaA family of radical *S*-adenosylmethionine enzymes and contains a characteristic conserved C*xxx*C*xx*C motif, to date, we have been unable to show that viperin binds iron. Both ^{55}Fe labeling of viperin-expressing yeast and heavy metal analysis of soluble recombinant viperin produced in insect cells showed no binding of iron or other heavy metals (data not shown). However, a previous study showed that mutating these three cysteines to alanines abolished the anti-HCV activity of viperin (8). It is possible that viperin binds Fe-S clusters weakly or transiently or that our expression systems were insufficient to detect metal binding to mammalian viperin. Alternatively, these cysteines may be critical for coordinating another, unknown activity. To further investigate these possibilities, future studies should examine such viperin mutants for antiviral activity against other viruses.

Acknowledgments—We thank Drs. David Stepensky and Jon Kagan for providing reagents, the late Dr. Marc Pypaert (Yale University) for assistance with immunoelectron microscopy, Dr. Roland Lill (Phillips University, Marburg, Germany) and Dr. Deborah Zamble (University of Toronto) for performing metal analyses, Nikhil Joshi and Dr. Xiuyan Wang for scientific advice, and Nancy Dometios for manuscript preparation.

REFERENCES

1. Katze, M. G., He, Y., and Gale, M., Jr. (2002) *Nat. Rev. Immunol.* **2,** 675–687
2. Haller, O., Kochs, G., and Weber, F. (2006) *Virology* **344,** 119–130
3. Chin, K. C., and Cresswell, P. (2001) *Proc. Natl. Acad. Sci. U. S. A.* **98,** 15125–15130
4. Wang, X., Hinson, E. R., and Cresswell, P. (2007) *Cell Host Microbe* **2,** 96–105
5. Helbig, K. J., Lau, D. T., Semendric, L., Harley, H. A., and Beard, M. R. (2005) *Hepatology* **42,** 702–710
6. Zhang, Y., Burke, C. W., Ryman, K. D., and Klimstra, W. B. (2007) *J. Virol.* **81,** 11246–11255
7. Rivieccio, M. A., Suh, H. S., Zhao, Y., Zhao, M. L., Chin, K. C., Lee, S. C., and Brosnan, C. F. (2006) *J. Immunol.* **177,** 4735–4741
8. Jiang, D., Guo, H., Xu, C., Chang, J., Gu, B., Wang, L., Block, T. M., and Guo, J. T. (2008) *J. Virol.* **82,** 1665–1678
9. Antonny, B. (2006) *Curr. Opin. Cell Biol.* **18,** 386–394

10. McMahon, H. T., and Gallop, J. L. (2005) *Nature* **438,** 590–596
11. Fukuda, M., Yamamoto, A., and Mikoshiba, K. (2001) *J. Biol. Chem.* **276,** 41112–41119
12. Yamamoto, A., Masaki, R., and Tashiro, Y. (1996) *J. Cell Sci.* **109,** 1727–1738
13. Snapp, E. L., Hegde, R. S., Francolini, M., Lombardo, F., Colombo, S., Pedrazzini, E., Borgese, N., and Lippincott-Schwartz, J. (2003) *J. Cell Biol.* **163,** 257–269
14. Peaper, D. R., Wearsch, P. A., and Cresswell, P. (2005) *EMBO J.* **24,** 3613–3623
15. Presley, J. F., Cole, N. B., Schroer, T. A., Hirschberg, K., Zaal, K. J., and Lippincott-Schwartz, J. (1997) *Nature* **389,** 81–85
16. Folsch, H., Pypaert, M., Maday, S., Pelletier, L., and Mellman, I. (2003) *J. Cell Biol.* **163,** 351–362
17. Orci, L., Brown, M. S., Goldstein, J. L., Garcia-Segura, L. M., and Anderson, R. G. (1984) *Cell* **36,** 835–845
18. Stephens, D. J., and Pepperkok, R. (2004) *J. Cell Sci.* **117,** 3635–3644
19. Dascher, C., and Balch, W. E. (1994) *J. Biol. Chem.* **269,** 1437–1448
20. Berger, J., Hauber, J., Hauber, R., Geiger, R., and Cullen, B. R. (1988) *Gene* (*Amst.*) **66,** 1–10
21. Calfon, M., Zeng, H., Urano, F., Till, J. H., Hubbard, S. R., Harding, H. P., Clark, S. G., and Ron, D. (2002) *Nature* **415,** 92–96
22. Zimmerberg, J., and Kozlov, M. M. (2006) *Nat. Rev. Mol. Cell Biol.* **7,** 9–19
23. Lee, M. C., Orci, L., Hamamoto, S., Futai, E., Ravazzola, M., and Schekman, R. (2005) *Cell* **122,** 605–617
24. Mackenzie, J. (2005) *Traffic* **6,** 967–977
25. Miller, S., and Krijnse-Locker, J. (2008) *Nat. Rev. Microbiol.* **6,** 363–374